Biophysics

Deutsche Ausgabe: DOI: 10.1002/ange.201508648
Internationale Ausgabe: DOI: 10.1002/anie.201508648

A Usual G-Protein-Coupled Receptor in Unusual Membranes

Udeep Chawla[+], Yunjiang Jiang[+], Wan Zheng, Liangju Kuang, Suchithranga M. D. C. Perera, Michael C. Pitman, Michael F. Brown, and Hongjun Liang**

Abstract: *G-protein-coupled receptors (GPCRs) are the largest family of membrane-bound receptors and constitute about 50 % of all known drug targets. They offer great potential for membrane protein nanotechnologies. We report here a charge-interaction-directed reconstitution mechanism that induces spontaneous insertion of bovine rhodopsin, the eukaryotic GPCR, into both lipid- and polymer-based artificial membranes. We reveal a new allosteric mode of rhodopsin activation incurred by the non-biological membranes: the cationic membrane drives a transition from the inactive MI to the activated MII state in the absence of high [H$^+$] or negative spontaneous curvature. We attribute this activation to the attractive charge interaction between the membrane surface and the deprotonated Glu134 residue of the rhodopsin-conserved ERY sequence motif that helps break the cytoplasmic "ionic lock". This study unveils a novel design concept of non-biological membranes to reconstitute and harness GPCR functions in synthetic systems.*

Membrane proteins are biologically derived high-performance materials that mediate matter transport, information processing, and energy conversion across nanoscale cellular boundaries, and pose great potential for bio-nanoengineering.[1] Bovine rhodopsin is a canonical prototype of G-protein-coupled receptors (GPCRs), the largest family of membrane proteins (MPs) in the human genome, and the most frequent drug targets.[2] Understanding GPCR activation mechanisms is far reaching in terms of GPCR-based biological signaling, as well as pharmaceutical development.[3] Here, we illustrate how GPCR activation is affected by specific allosteric interactions in the case of visual rhodopsin. For bio-nanotechnologies, the broad utility of GPCRs is limited by the fluidic and labile nature of biomembranes. Putting GPCRs to work faces two upmost unanswered challenges: 1) how to reconstitute GPCRs in robust and scalable synthetic membranes, and 2) how does the non-biological membrane affect the activities of GPCRs?

Conventional methods of reconstituting MPs rely critically on detergent solubilization or sonication forces to destabilize membranes, followed by external removal of detergent; this eventually drives a transition from MP-detergent-membrane micelles to proteomembranes.[4] The utility of this approach for robust, non-fluidic membranes resisting such destabilization is unclear. A new, charge-interaction-directed reconstitution (CIDR) paradigm[5] was proposed to induce preferential contact between a MP hydrophilic domain and the membrane by charge attraction, which triggers MP insertion and decortication of detergent micelles associated with the MP hydrophobic domain. Formation of proteomembranes occurs spontaneously without needing external means for detergent removal.[5] CIDR of functional proteorhodopsin[5,6] and bacterial reaction center,[7] the two prokaryotic MPs differing greatly in structural complexity, has been reported in both lipid- and polymer-based membranes, even when the membranes are in an entangled or "frozen" state with greatly enhanced stability. While proton pumping kinetics mediated by proteorhodopsin are allosterically slowed down as the polymer membrane block size increases and flexibility decreases,[6] reaction center-mediated electron-transport kinetics appear insensitive.[7] These studies suggest the broad utility of CIDR for developing robust and scalable MP-based bio-nanotechnologies, potentially including eukaryotic GPCRs.

We show that CIDR indeed induces spontaneous and functional reconstitution of bovine rhodopsin into both lipid- and polymer-based artificial membranes that differ greatly from retinal disk membranes (RDM) in terms of lipid composition and charge state, both of which are regarded to play crucial roles in rhodopsin activation.[8] Native RDM contain primarily lipids with phosphocholine (PC), phosphoethanolamine (PE), and phosphoserine (PS) headgroups with 47 % docosahexaenoic acid (22:6ω3) acyl chains. The mechanistic roles of these lipids are explained by 1) the flexible surface model (FSM),[8d,e] which proposes that the negative spontaneous curvature of PE lipids helps offset the solvation energy cost at the protein–lipid–water interface of activated MII;[8a–g] 2) high [H$^+$] condensed on the membrane surface because of negatively charged PS lipids, which shifts the MI–MII equilibrium toward MII;[8i–l] and 3) specific lipid–rhodopsin interactions,[8g,h] such as H bonding between PE headgroups and newly exposed protein residues upon MII

[*] U. Chawla,[+] S. M. D. C. Perera, Dr. M. C. Pitman, Prof. Dr. M. F. Brown
Department of Chemistry & Biochemistry
Department of Physics University of Arizona
Tucson, AZ 85721 (USA)
E-mail: mfbrown@u.arizona.edu
Y. Jiang,[+] W. Zheng, L. Kuang, Prof. Dr. H. Liang
Department of Metallurgical & Materials Engineering
Colorado School of Mines, Golden, CO 80401 (USA)
Y. Jiang,[+] Prof. Dr. H. Liang
Current address:
Department of Cell Physiology and Molecular Biophysics
Center for Membrane Protein Research
Texas Tech, University Health Science Center
Lubbock, TX 79430 (USA)
E-mail: H.liang@ttuhsc.edu
[+] These authors contributed equally to this work.

Supporting information, including experimental details on the synthesis of artificial membranes, purification of bovine rhodopsin, CIDR of proteomembranes, and their structural and functional characterizations, for this article is available on the WWW under http://dx.doi.org/10.1002/anie.201508648.

formation.[8g] We reveal here a completely new mode of rhodopsin activation in non-biological membranes that does not fit into any of these mechanisms (Figure 1).

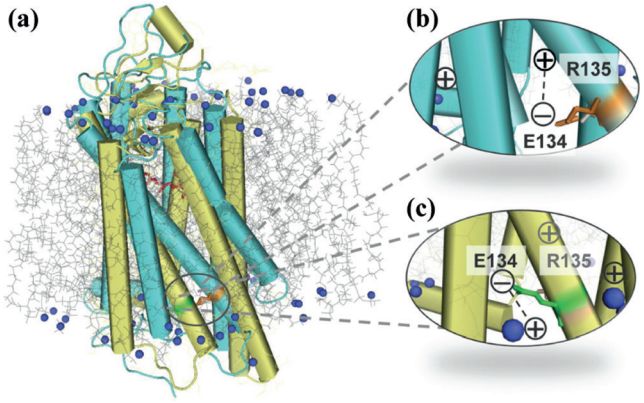

Figure 1. Cationic membrane surface moieties activate rhodopsin. a) Photoactivation of rhodopsin characterized by a conformation shift from the dark state (1U19; blue) to the activated MII state (3PXO; yellow). b) Cytoplasmic "ionic lock" (i.e. Glu134-Arg135 salt bridge) in the dark state. c) Attractive charge interaction between cationic membrane surface moieties (green dots) and deprotonated Glu134 helps break the "ionic lock".

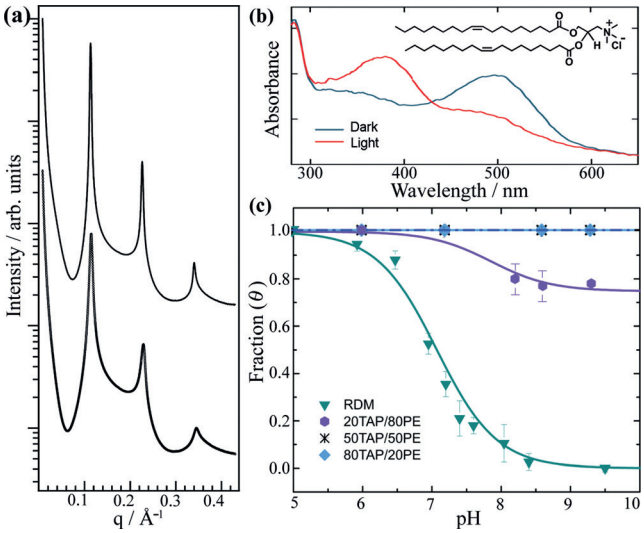

Figure 2. Spontaneous CIDR of rhodopsin in DOTAP/DOPE membranes. a) Synchrotron SAXS (25 °C) of proteoliposome complexes comprised of rhodopsin and 80/20 (top) or 20/80 (bottom) DOTAP/DOPE. b) UV/Vis spectra of rhodopsin in 80/20 DOTAP/DOPE upon photoactivation (25 °C). c) pH titration traces of rhodopsin in different membranes (10 °C). The structure of DOTAP is shown as inset to panel (b); see the Supporting Information for additional lipid structures.

We first examined CIDR of bovine rhodopsin in lipid-based artificial membranes with negative spontaneous curvature. Since rhodopsin has an isoelectric point of 6.2[9] and is overall anionically charged at physiological pH, we chose 1,2-dioleoyl-3-trimethylammonium-propane (DOTAP), a non-biological cationic lipid, and mixed it with zwitterionic 1,2-dioleoyl-*sn*-glycero-3-phosphoethanolamine (DOPE). Unlike DOPE, the DOTAP has zero spontaneous curvature.[10] We prepared three model membranes, 80/20, 50/50, and 20/80 DOTAP/DOPE, respectively, with increasing negative membrane curvature. The CIDR of bovine rhodopsin solubilized by *n*-dodecyl-β-D-maltoside (DDM) into all model DOTAP/DOPE membranes triggers a spontaneous transition from free-suspending spherical liposomes to a condensed phase of proteoliposome complexes (see the Supporting Information). Synchrotron small-angle X-ray scattering (SAXS) of all complexes revealed equally spaced harmonics characteristic of a multilamellar structure. As an example shown in Figure 2a, the first scattering peak (q_{001}) is centered at 0.113 and 0.114 Å^{-1}, respectively, for 80/20 and 20/80 DOTAP/DOPE, indicating a proteomembrane lamellar periodicity of 55–56 Å similar to the transmembrane dimension of reconstituted proteorhodopsin as previously reported.[5a,b] This lamellar periodicity does not support the presence of DDM micelles either with the membrane or bovine rhodopsin. The maximum possible residual DDM after re-dispersing the condensed proteomembrane complexes in a detergent-free buffer for functional characterization is negligible (see the Supporting Information).

Photoactivation of rhodopsin involves breaking two "ionic locks" accompanied by a series of spectroscopically distinct photointermediates:[11] starting from the dark state (A_{max} = 500 nm), retinal isomerization leads to MI formation (A_{max} = 480 nm). Subsequent disruption of the first interhelical "ionic lock" by internal proton transfer from the retinal protonated Schiff base (PSB) to its counterion, Glu113, on the extracellular side of rhodopsin leads to MII_a formation (A_{max} = 380 nm). Although a blue shift of the UV/Vis absorption maximum (500→380 nm) is a strong indication of rhodopsin activation, only disruption of the second "ionic lock" between Glu134 and Arg135 of the rhodopsin-conserved ERY sequence motif puts the protein in the activated MII_b state (A_{max} = 380 nm), as it is associated with the motion of transmembrane helix 6 (TM6) that sets the helix-loop conformation for transducin interaction. This second unlocking event, as assessed by FTIR and EPR spectroscopy,[11d,e] gives rise to the pH dependence of the MI–MII equilibrium favoring fully active MII_bH^+ at acidic pH, because protonation of Glu134 is enthalpically downhill.

Given the favorable role of negative membrane spontaneous curvature on rhodopsin activation,[8a–g] we expect to observe a shift of the MI–MII equilibrium toward MII at increasing DOPE concentration. What we actually observed is completely on the contrary. The UV/Vis spectra of rhodopsin in all DOTAP/DOPE membranes upon photoactivation (measured at pH 6.9 and room temperature) revealed a similar blue shift of the absorption maximum (Figure 2b), indicative of MII formation that is independent of membrane curvature. To determine the pH-dependent equilibrium between inactive MI and activated MII, we performed pH titration studies of all proteoliposome complexes at 10 °C. It has been shown[11e,i] that at 10 °C all MII observed by UV/Vis spectra is the active MII observed by FTIR spectroscopy. The contribution of the activated MII state to the photoproduct equilibrium (θ) was determined

from the photoproduct minus dark state UV/Vis difference spectra, fit with the Henderson–Hasselbalch function when possible (Supporting Information), and plotted as a function of pH (Figure 2c). The pH titration curve of native rhodopsin in RDM at 10 °C is also plotted as a comparison. Surprisingly, for proteoliposome membranes with low negative spontaneous curvature, that is, 80/20 DOTAP/DOPE, which should deter MII formation and shift the transition to more acidic pH as compared to RDM, we observed no transition at all. Instead, 100 % activated MII was observed in the entire pH range (5–10) that we tested. The same behavior was true for 50/50 DOTAP/DOPE. When the negative membrane curvature is further increased (i.e. 20/80 DOTAP/DOPE), however, we observed a transition at alkaline pH, albeit with a non-zero end-point value indicating 80 % photoproduct was still in the activated MII state. This observation is not consistent with previous explanations for rhodopsin activation involving negative membrane curvature,[8a–g] and suggests an additional activation mechanism despite the unfavorable solvation energy costs at the protein–lipid–water interface.

One possible player is the cationic lipid DOTAP shown in Figure 2 (inset). To reduce or eliminate the contribution from negative spontaneous curvature and specific DOPE-rhodopsin interactions[8g] to rhodopsin activation, we replaced DOPE with zwitterionic 1,2-dioleoyl-*sn*-glycero-3-phosphocholine (DOPC), and prepared a series of DOTAP/DOPC membranes with increasing membrane charge density, that is, 20/80, 50/50, 80/20, and 100/0 DOTAP/DOPC, respectively. Like DOTAP, the DOPC also has zero spontaneous curvature.[10b] We observed spontaneous CIDR of DDM-solubilized bovine rhodopsin into all DOTAP/DOPC membranes to form condensed proteoliposome complexes, and synchrotron SAXS studies of these complexes revealed a multilamellar structure. As an example shown in Figure 3a, the first scattering peak (q_{001}) is centered at 0.110 and 0.111 Å^{-1}, for 20/80 and 80/20 DOTAP/DOPC, respectively, indicating a proteomembrane lamellar periodicity of 56–57 Å similar to that observed in the DOTAP/DOPE system.

Planar lipid membranes such as DOPC favor the inactive rhodopsin MI state under physiological pH (ca. 7–8),[8a–g] and anionic membrane surface potential favors the activated rhodopsin MII state because condensed high [H$^+$] on the membrane surface facilitates protonation of Glu134, which shifts the MI–MII equilibrium toward MII.[8i–l] Taken together, cationic and planar DOTAP/DOPC membranes should strongly favor the MI state, because the cationic membrane surface potential would have an opposite effect. What we observed is, again, completely on the contrary. The UV/Vis spectra of rhodopsin in all DOTAP/DOPC membranes upon photoactivation showed similar MII formation (Figure 3b). In addition pH titration studies of proteoliposome complexes at 10 °C (Figure 3c) clearly show that all DOTAP/DOPC membranes favor the rhodopsin MII state even at alkaline pH, and acid denaturation controls (A_{max} = 440 nm) indicate a PSB rather than free retinal (A_{max} = 383 nm; Supporting Information). Consistent with what is observed in the DOTAP/DOPE system, the higher the percentage of DOTAP in the membranes, the higher the fraction of activated MII state. When DOTAP reaches 80 % or more, the alkaline end point is unity, thus revealing fully active MII in the entire pH range (5–10).[11e]

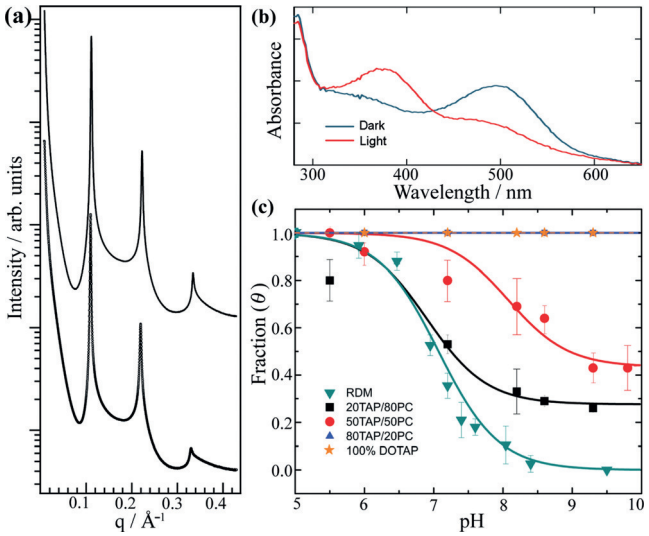

Figure 3. Spontaneous CIDR of rhodopsin in DOTAP/DOPC membranes. a) Synchrotron SAXS (25 °C) of proteoliposome complexes comprised of rhodopsin and 80/20 (top) or 20/80 (bottom) DOTAP/DOPC. b) UV/Vis spectra of rhodopsin in 80/20 DOTAP/DOPC upon photoactivation (25 °C). c) pH titration traces of rhodopsin in different membranes (10 °C).

The role of DOTAP on activating rhodopsin could be attributed to specific DOTAP-rhodopsin interactions yet to be identified, or to its cationic membrane surface. To rule out the contribution from specific DOTAP-rhodopsin interactions, and to test the broad utility of CIDR on reconstituting the eukaryotic GPCR in robust and scalable synthetic membranes, we synthesized a well-defined amphiphillic triblock copolymer by atom-transfer radical polymerization, polybutadiene$_{35}$-*b*-(poly(4-vinyl-*N*-methylpyridine iodide)$_{30}$)$_2$, that is, PBD$_{35}$-*b*-(P4MVP$_{30}$)$_2$ (Supporting Information, also see the inset of Figure 4b for its structure). Unlike polymeric surfactants such as NVoy, SMAs, and Amphipols that are used to solubilize MPs,[12] the amphiphilic triblock copolymer self-assembles in water into liposome-like polymersomes (Supporting Information, also see the inset of Figure 4a) with a cationic membrane charge density that is an order of magnitude higher than DOTAP membranes.[5c] Due to the symmetric structure of the triblock copolymer, the polymersome membrane has zero spontaneous curvature.

We observed, for the first time, spontaneous CIDR of the eukaryotic GPCR in the robust synthetic block copolymer membranes. Synchrotron SAXS of the proteopolymersomes revealed three equally spaced harmonics characteristic of a multilamellar structure (marked by arrows, Figure 4a). The scattering is not as sharp as that of proteoliposomes, most likely due to a more diffusive hydrophilic-hydrophobic interface. The first scattering peak (q_{001}) is centered at 0.107 Å^{-1}, indicating a proteomembrane lamellar periodicity of 59 Å. Despite that rhodopsin is reconstituted in an entirely synthetic polymer membrane without any lipid component, UV/Vis spectra of the proteopolymer membranes upon photoactivation still revealed MII formation (Figure 4b),

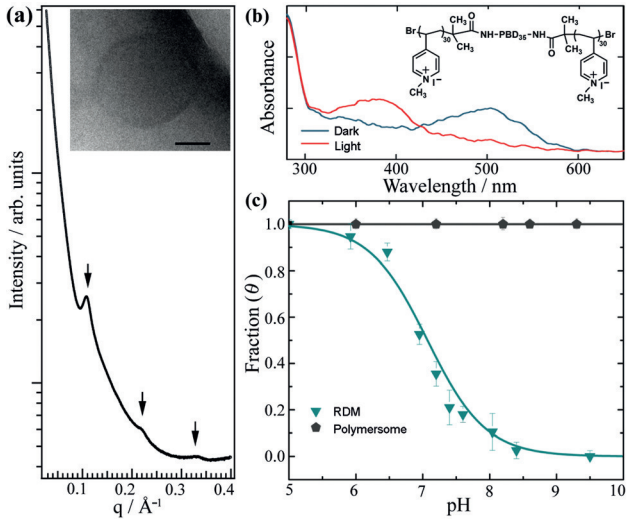

Figure 4. Spontaneous CIDR of rhodopsin in amphiphilic block copolymer membranes. a) Synchrotron SAXS (25 °C) of proteopolymersome complexes comprised of rhodopsin and PBD_{35}-*b*-$(P4MVP_{30})_2$. b) UV/Vis spectra of rhodopsin in proteopolymer membrane upon photoactivation (25 °C). c) pH titration of rhodopsin in different membranes (10 °C). A transmission electron microscope (TEM) picture of polymersome (scale bar: 50 nm) and structure of PBD_{35}-*b*-$(P4MVP_{30})_2$ are shown as insets in panels (a) and (b), respectively.

and pH titration at 10 °C (Figure 4c) confirmed fully active MII with an alkaline end point unity in the entire pH range (5–10). It becomes clear that the cationic membrane surface charge is associated with a new mode of rhodopsin activation: the higher the cationic membrane surface charge density, the higher the fraction of activated MII state in the photoproduct equilibrium.

We attribute this new mode of activation to the attractive charge interaction between the membrane and the deprotonated Glu134 residue of the rhodopsin-conserved ERY sequence motif that helps break the cytoplasmic "ionic lock" (Figure 1). To further investigate cationic stabilization of Glu134, we also conducted a new analysis of microsecond-scale molecular dynamics (MD) simulations of bovine rhodopsin in a realistic biomembrane model (Supporting Information). The major new finding shows that Glu134 may form direct salt bridges with membrane-supported cationic moieties through a channel opening between TM4 and TM5. Because Glu134 is situated at the interface between the lipid bilayer and the aqueous phase,[11c] the ERY ionic lock can be affected by charge neutralization involving cationic lipids or polymersomes. Our MD simulations are consistent with previous FTIR studies[11g] and X-ray structural data for active rhodopsin[13] (Supporting Information). Photoactivation of rhodopsin involves breaking two "ionic locks" accompanied by a conformational change to dock transducin.[11] At low temperature ($\leq$ 10 °C), release of both "ionic locks" are coupled, in that protonation of Glu134 helps offset the free-energy costs associated with breaking the first "ionic lock", whereas at higher temperature release of both "ionic locks" becomes partially uncoupled.[11e] A release of both "ionic locks" is required for full receptor activation, but the activating movement of TM6 is independent of H^+ uptake by Glu134. Our data suggest that in synthetic systems, the role of H^+ can be replaced with cationic membrane surface moieties positioned in close proximity to Glu134 on the rhodopsin-conserved ERY sequence motif.[14] In support of this interpretation, we have also carried out ATR-FTIR measurements of the light-induced binding of a high-affinity transducin peptide to rhodopsin in DOTAP versus the RDM control (Supporting Information). For the ATR-FTIR measurements, a light-induced difference signal is obtained due to structural changes of the MII/peptide complex, including protonation of Glu134 in the transducin-bound state.[11g] The difference signal is attributed to the "extra MII"[15] because of the active MII_bH^+ state. Active MII is produced and in each case the spectral difference entails destabilization of the ionic lock because of Glu134 of the E(D)RY sequence motif.[11e] Hence we conclude that DOTAP, polymerosomes, and the high-affinity transducin peptide all exert their actions by stabilizing the active $MIIH^+$ state, in which the ionic lock involving Glu134 of the E(D)RY sequence motif is broken giving "extra MII".

In summary, we report here for the first time the broad utility of CIDR for inducing spontaneous and functional reconstitution of bovine rhodopsin, a canonical prototype of eukaryotic GPCRs. The CIDR makes it possible to prepare robust and scalable proteomembrane arrays in both 3D and 2D[16] by spontaneous self- and directed-assembly processes amenable to many engineering systems. We further show that photoactivation of rhodopsin proceeds in robust synthetic polymer membranes without any biological lipid component. Finally, we discovered a new mode of rhodopsin activation triggered by the attractive charge interaction between the membrane and the deprotonated Glu134 residue of the rhodopsin-conserved ERY sequence motif. We expect that the role of H^+ at the membrane interface under physiological conditions is replaceable by a wide range of cationic membrane surface moieties in synthetic systems, which form ionic bonds with Glu134 and provide a similarly favorable thermodynamic driving force to shift the MI–MII equilibrium toward activated MII. Given that Glu134 in rhodopsin is part of a highly conserved triad, D(E)RY, our study implies that the observed effect will be transferrable to other rhodopsin-like GPCRs in synthetic systems.

Acknowledgements

This work was supported by NSF through DMR-1410825 and CBET-1160291 (H.L.), and by NIH (M.F.B.). We thank Total USA for providing the PBD samples. SAXS experiments were performed at the SSRL. Use of the SSRL, SLAC National Accelerator Laboratory, is supported by the U.S. Department of Energy, Office of Science, Office of Basic Energy Sciences under contract number DE-AC02-76SF00515. The SSRL Structural Molecular Biology Program is supported by the DOE Office of Biological and Environmental Research, and by the National Institutes of Health, National Institute of General Medical Sciences (including P41GM103393). The contents of this publication are solely

the responsibility of the authors and do not necessarily represent the official views of NIGMS or NIH.

Keywords: biophysics · flexible surface model · G-protein-coupled receptor · photoactivation · rhodopsin

How to cite: *Angew. Chem. Int. Ed.* **2016**, *55*, 588–592
Angew. Chem. **2016**, *128*, 598–602

[1] a) V. Subramaniam, I. D. Alves, G. F. J. Salgado, P.-W. Lau, R. J. Wysocki, Z. Salamon, G. Tollin, V. J. Hruby, M. F. Brown, S. S. Saavedra, *J. Am. Chem. Soc.* **2005**, *127*, 5320–5321; b) R. Michel, V. Subramaniam, S. L. McArthur, B. Bondurant, G. D. D'Ambruoso, H. K. Hall, Jr., M. F. Brown, E. E. Ross, S. S. Saavedra, D. G. Castner, *Langmuir* **2008**, *24*, 4901–4906; c) V. Subramaniam, G. D. D'Ambruoso, H. K. Hall, Jr., R. J. Wysocki, Jr., M. F. Brown, S. S. Saavedra, *Langmuir* **2008**, *24*, 11067–11075; d) E. Reimhult, K. Kumar, *Trends Biotechnol.* **2008**, *26*, 82–89; e) P. Curnow, *Biochem. Soc. Trans.* **2009**, *37*, 643–652.

[2] a) M. C. Lagerström, H. B. Schiöth, *Nat. Rev. Drug Discovery* **2008**, *7*, 339–357; b) R. Nygaard, T. M. Frimurer, B. Holst, M. M. Rosenkilde, T. W. Schwartz, *Trends Pharmacol. Sci.* **2009**, *30*, 249–259; c) D. M. Rosenbaum, S. G. F. Rasmussen, B. K. Kobilka, *Nature* **2009**, *459*, 356–363; d) G. Khelashvili, P. B. C. Albornoz, N. Johner, S. Mondal, M. Caffrey, H. Weinstein, *J. Am. Chem. Soc.* **2012**, *134*, 15858–15868; e) R. C. Stevens, V. Cherezov, V. Katritch, R. Abagyan, P. Kuhn, H. Rosen, K. Wüthrich, *Nat. Rev. Drug Discovery* **2013**, *12*, 25–34.

[3] a) X. Deupi, *Biochim. Biophys. Acta Bioenerg.* **2014**, *1837*, 674–682; b) S. Wolf, S. Grünewald, *Plos One* **2015**, *10*, e0123533.

[4] a) K. Hong, P. J. Knudsen, W. L. Hubbell, *Methods Enzymol.* **1982**, *81*, 144–150; b) J. L. Rigaud, D. Levy, *Methods Enzymol.* **2003**, *372*, 65–86; c) X. Y. Zhang, P. Tanner, A. Graff, C. G. Palivan, W. Meier, *J. Polym. Sci. Part A* **2012**, *50*, 2293–2318.

[5] a) H. Liang, G. Whited, C. Nguyen, G. D. Stucky, *Proc. Natl. Acad. Sci. USA* **2007**, *104*, 8212–8217; b) H. Liang, G. Whited, C. Nguyen, A. Okerlund, G. D. Stucky, *Nano Lett.* **2008**, *8*, 333–339; c) D. Hua, L. Kuang, H. Liang, *J. Am. Chem. Soc.* **2011**, *133*, 2354–2357.

[6] L. Kuang, D. A. Fernandes, M. O'Halloran, W. Zheng, Y. Jiang, V. Ladizhansky, L. S. Brown, H. Liang, *ACS Nano* **2014**, *8*, 537–545.

[7] L. Kuang, T. L. Olson, S. Lin, M. Flores, Y. Jiang, W. Zheng, J. C. Williams, J. P. Allen, H. Liang, *J. Phys. Chem. Lett.* **2014**, *5*, 787–791.

[8] a) N. J. Gibson, M. F. Brown, *Photochem. Photobiol.* **1991**, *54*, 985–992; b) N. J. Gibson, M. F. Brown, *Biochemistry* **1993**, *32*, 2438–2454; c) M. F. Brown, *Curr. Top. Membr.* **1997**, *44*, 285–356; d) A. V. Botelho, N. J. Gibson, R. L. Thurmond, Y. Wang, M. F. Brown, *Biochemistry* **2002**, *41*, 6354–6368; e) M. F. Brown, *Biochemistry* **2012**, *51*, 9782–9795; f) W. E. Teague, Jr., O. Soubias, H. Petrache, N. Fuller, K. G. Hines, R. P. Rand, K. Gawrisch, *Faraday Discuss.* **2013**, *161*, 383–395; g) O. Soubias, W. E. Teague, Jr., K. G. Hines, D. C. Mitchell, K. Gawrisch, *Biophys. J.* **2010**, *99*, 817–824; h) A. Grossfield, S. E. Feller, M. C. Pitman, *Proc. Natl. Acad. Sci. USA* **2006**, *103*, 4888–4893; i) F. C. Tsui, S. A. Sundberg, W. L. Hubbell, *Biophys. J.* **1990**, *57*, 85–87; j) F. DeLange, M. Merkx, P. H. M. Bovee-Geurts, A. M. A. Pistorius, W. DeGrip, *Eur. J. Biochem.* **1997**, *243*, 174–180; k) S. K. Gibson, J. H. Parkes, P. A. Liebman, *Biochemistry* **1999**, *38*, 11103–11114; l) Y. Wang, A. V. Botelho, G. V. Martinez, M. F. Brown, *J. Am. Chem. Soc.* **2002**, *124*, 7690–7701.

[9] a) J. J. Plantner, E. L. Kean, *Biochim. Biophys. Acta* **1983**, *744*, 312–319; b) W. L. Hubbell, *Biophys. J.* **1990**, *57*, 99–108.

[10] a) I. Koltover, T. Salditt, J. O. Radler, C. R. Safinya, *Science* **1998**, *281*, 78–81; b) J. O. Radler, I. Koltover, T. Salditt, C. R. Safinya, *Science* **1997**, *275*, 810–814.

[11] a) S. Arnis, K. P. Hofmann, *Proc. Natl. Acad. Sci. USA* **1993**, *90*, 7849–7853; b) J. M. Kim, C. Altenbach, M. Kono, D. D. Oprian, W. L. Hubbell, H. G. Khorana, *Proc. Natl. Acad. Sci. USA* **2004**, *101*, 12508–12513; c) X. Periole, M. A. Ceruso, E. L. Mehler, *Biochemistry* **2004**, *43*, 6858–6864; d) B. Knierim, K. P. Hofmann, O. P. Ernst, W. L. Hubbell, *Proc. Natl. Acad. Sci. USA* **2007**, *104*, 20290–20295; e) M. Mahalingam, K. Martínez-Mayorga, M. F. Brown, R. Vogel, *Proc. Natl. Acad. Sci. USA* **2008**, *105*, 17795–17800; f) R. Vogel, M. Mahalingam, S. Luedke, T. Huber, F. Siebert, T. P. Sakmar, *J. Mol. Biol.* **2008**, *380*, 648–655; g) K. Fahmy, T. P. Sakmar, F. Siebert, *Biochemistry* **2000**, *39*, 10607–10612; h) E. Zaitseva, M. F. Brown, R. Vogel, *J. Am. Chem. Soc.* **2010**, *131*, 4815–4821; i) M. F. Brown, *Methods Mol. Biol.* **2012**, *914*, 127–153.

[12] a) C. Klammt, M. H. Perrin, I. Maslennikov, L. Renault, M. Krupa, W. Kwiatkowski, H. Stahlberg, W. Vale, S. Choe, *Protein Sci.* **2011**, *20*, 1030–1041; b) T. J. Knowles, R. Finka, C. Smith, Y. P. Lin, T. Dafforn, M. Overduin, *J. Am. Chem. Soc.* **2009**, *131*, 7484–7485; c) C. Tribet, R. Audebert, J. L. Popot, *Proc. Natl. Acad. Sci. USA* **1996**, *93*, 15047–15050.

[13] H.-W. Choe, Y. J. Kim, J. H. Park, T. Morizumi, E. F. Pai, N. Krauss, K. P. Hofmann, P. Scheerer, O. P. Ernst, *Nature* **2011**, *471*, 651–656.

[14] U. Chawla, W. Zheng, L. J. Kuang, Y. J. Jiang, S. M. D. C. Perera, M. F. Brown, H. J. Liang, *Biophys. J.* **2015**, *108*, 500a–501a.

[15] K. P. Hofmann, P. Scheerer, P. W. Hildebrand, H. W. Choe, J. H. Park, M. Heck, O. P. Ernst, *Trends Biochem. Sci.* **2009**, *34*, 540–552.

[16] K. Ataka, F. Giess, W. Knoll, R. Naumann, S. Haber-Pohlmeier, B. Richter, J. Heberle, *J. Am. Chem. Soc.* **2004**, *126*, 16199–16206.

Received: September 15, 2015
Revised: November 2, 2015
Published online: December 3, 2015

